ScienSage

Journal of Advanced Scientific Research

Available online through http://www.sciensage.info

ISSN
0976-9595
Research Article

# SYNTHESIS, X-RAY CRYSTALLOGRAPHY, HIRSHFELD SURFACE AND 3D ENERGY FRAMEWORK ANALYSIS OF TWO IMIDAZOLE DERIVATIVES

**G. Dhanalakshmi[1], Ramanjaneyulu Mala[2,3], Dhakshinamurthy Divya[2], Sathiah Thennarasu[2,3], S. Aravindhan*[1]**

[1]*Department of Physics, Presidency College (Autonomous), University of Madras, Chennai, India*

[2]*Organic & Bioorganic Chemistry Laboratory, CSIR-Central Leather Research Institute Adyar, Chennai, India*

[3]*Academy of Scientific and Innovative Research (AcSIR), CSIR-Central Leather Research Institute Adyar, Chennai, India*

*India.*Corresponding author: aravindhanpresidency@gmail.com*

## ABSTRACT

Heterocyclic compounds play an important role in organic chemistry due to their wide variety of applications in pharmacy, veterinary science and agriculture. Many significant heterocycles having application in medicinal chemistry and material science has nitrogen fused heterocyclic imidazole ring as common structural motifs. Imidazoles are one among the heterocyclic compounds which show significant pharmacological properties. Due to the importance of imidazole derivatives two compounds2-(5-(3-(tert-butylamino)imidazo[1,2-a]pyridin-2-yl)thiophen-2-yl)-6-fluoro-benzaldehyde and Methyl-3-(tert-butylamino)-2-(pyridin-2-yl)imidazo[1,2-a]pyridine-8-carboxylate has been synthesized, and the structures were confirmed by single crystal X-ray diffraction studies. In the crystals, molecules are linked by intermolecular C-H…S, N-H…N, and C-H…N hydrogen bonds. Both compounds exhibits π..π, and C-H…π interactions. Hirshfeld surface analysis revealed that in both compounds H…H interactions have the major contribution to the molecular surface. From the energy framework analysis, it was found that the dispersion components have a major contribution in crystal.

**Keywords:** Crystal structure, imidazole, Hirshfeld surface analysis, Energy framework

## 1. INTRODUCTION

Heterocyclic compounds play an important role in organic chemistry due to their wide variety of applications in pharmacy, veterinary science and agriculture. Many significant heterocycles having application in medicinal chemistry and material science has nitrogen fused heterocyclic imidazole ring as common structural motifs. Imidazole are heterocyclic compounds which show important pharmacological and biochemical properties [1-4]. These derivatives exhibits anti-fungal [5], anti-bacterial [6], anti-tumor [7-8], anti-protozoal [9], anti-herpes [10], anti-inflammatory [11], anti-ulcerative, anti-hypertensive, anti-histaminic, and anti-helminthic properties [12]. These compounds are highly active against human cytomegalovirus and varicella-zoster virus [13]

Biological activities against various microorganisms [14-15], have been described for heterocyclic compounds of nitrogen. Literature survey reveals that they behave as amphoteric and possesses increased reactivity towards electrophilic attack [16]. It shows high stability to thermal, acid, base, oxidation and reduction conditions. It exists in two equivalent tautomeric forms because the hydrogen atom can be located on either of the two nitrogen atoms [17]. Imidazole can also be found in various compounds which are used for photography [18-19], and these derivatives are used as dopants for doping an organic semiconductor matrix material, organic semiconductor materials and electronic or optoelectronic structural elements [20-21]. Because of all these wide range of applications in this present work we report the synthesis, crystal structure, Hirshfeld surface and 3D energy framework analysis of the compounds.

## 2. EXPERIMENTAL

### 2.1. Synthesis of compound I

**2-(5-bromothiophen-2-yl)-N-(tert-butyl) imidazo[1,2-a]pyridin-3-amine (1A)** was prepared by our previous report [22a, 22b] with starting compounds as 2-aminopyridine, 5-bromothiophene-2-carbaldehyde and tertiary butyl isocyanide in Ethanol

solvent and finally added $I_2$ catalyst. Compound **1A** was purified by column chromatography by using 100-200 mesh silica as stationary phaseand hexane: ethyl acetate (60:40) mobile phase.

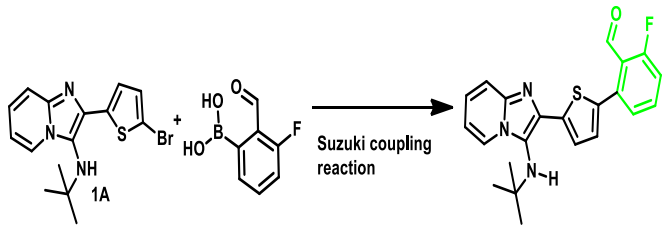


**2-(5-(3-(tert-butylamino)imidazo[1,2-a]pyridin-2-yl)thiophen-2-yl)-6-fluorobenzaldehyde** (1), In this experiment, ethyl thiophene-2-carboxylate (1) (27.4 mmol, 4.28 g), 1-bromo-4-(dodecyloxy) benzene (2) (13.7 mmol, 4.68 g) were dissolved in anhydrous dimethylacetamide (DMAc) (40 mL), potassium carbonate ($K_2CO_3$) (1.5 equiv, 411.5 mmol, 2.682g), palladium acetate ($Pd(OAc)_2$) (4 mol %, 54.8 mmol, 123 mg), tricyclohexylphosphinetetrafluoroborate (PCy3. HBF4) (8 mol %, 1.96 mmol, 400 mg) and pivalic acid (30 mol %, 4.1 mmol, 419 mg) added under nitrogen atmosphere. The reaction was maintained in a nitrogen atmosphere for 16 hours at 110°C and checked the progress of the reaction by TLC after the mixture was allowed to cool to room temperature. The obtained crude compound was dissolved in dichloromethane (DCM) 100 mL and washed with water the organic layer was collected and the solvent was removed by rotavapor. The resultant semisolid was purified by column chromatography using hexane and ethyl acetate as eluent (1:10). The ester compound was recrystallized in hot methanol. The white crystalline compound was obtained.

## 2.2. Synthesis of compound II

The final compound was prepared by our previous report [22c] with starting compound as methyl 2-aminonicotinate, picolinaldehyde and *tert*-butyl isocyanide in Ethanol solvent finally adding $I_2$ catalyst. The final compound was purified by column chromatography using 100-200 mesh silica as stationary phaseand hexane: ethyl acetate (60:40) mobile phase.

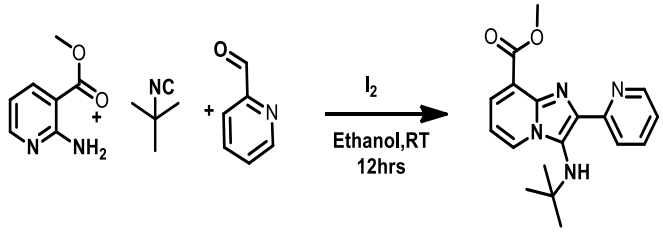


## 2.3. X-Ray Data collection, structure refinement and solution

Single crystal of the size 0.300 x 0.250 x 0.200 $mm^3$ were taken for data collection using Brukeraxs kappa Apex2 CCD Diffractometer at 296K with graphite monochromatic $MoK_\alpha$ radiation ($\lambda$= 0.71073 Å). Data was corrected for Lorentz-polarization and absorption factors. The structure was solved by direct methods using SHELXT-2014/4 [23], and refined using *SHELXL2014*/7 [24], by full matrix least squares on $F^2$. All non-hydrogen atoms were refined anisotropically and H atoms were localized from the difference electron-density maps and refined as riding atoms with C-H = 0.93 or 0.97 A° with $U_{iso}(H) = 1.5U_{eq}(C)$ for methyl H atoms and $1.2U_{eq}(C)$ for other H atoms. The program PLATON [25] was used for geometrical calculations. The software *MERCURY* [26] was used to generate packing diagrams.

The molecular structure of compound I and compound II are shown in Fig. 1 and Fig 2. The parameters for data collection and structure refinement of the compound I and II are listed in Table 1.

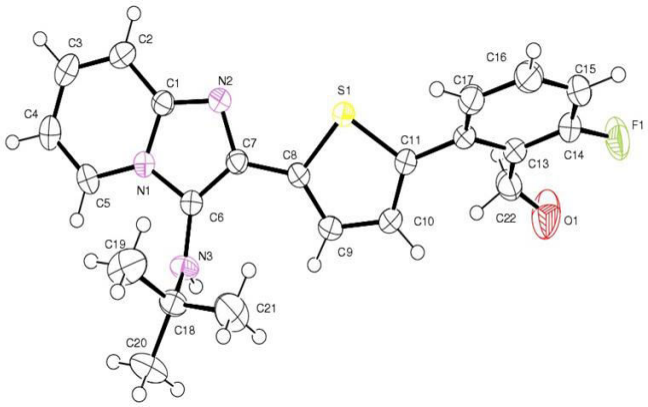


**Fig. 1: The ORTEP diagram of the compound I with the atom labeling. Displacement ellipsoids are drawn at the 40% probability level**

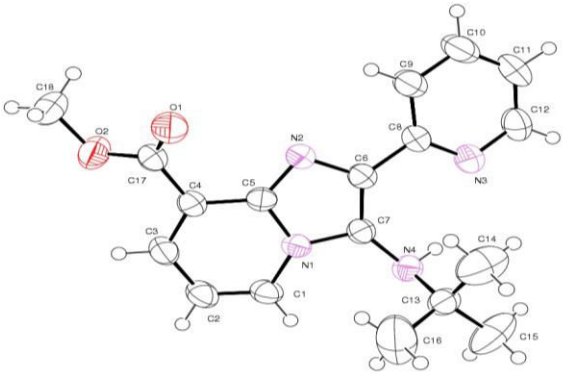


**Fig. 2: The ORTEP diagram of the compound II with the atom labeling. Displacement ellipsoids are drawn at the 40% probability level**

**Table 1: parameters for data collection and structure refinement of the compound I and II**

| PARAMETER | Compound I | Compound II |
|---|---|---|
| Empirical formula | $C_{22}H_{21}FN_3OS$ | $C_{18}H_{20}N_4O_2$ |
| Formula weight | 394.48 g/mol | 324.38 g/mol |
| Temperature | 296(2) K | 296(2) K |
| Wavelength | 0.71073 Å | 0.71073 Å |
| Crystal system | triclinic | monoclinic |
| Space group | P -1 | P 1 21/n 1 |
| Unit cell dimensions | a = 6.6255(2) Å α = 108.3250(13)° b = 10.2436(3) Å β = 93.8678(12)° c = 14.8236(4) Å γ = 92.4051(13)° | a = 9.9038(6) Å α = α = 90°° b = 10.3291(5) Å β = 101.315(2)°° c = 16.8669(8) Å γ = 90°° |
| Volume | 950.75(5) $Å^3$ | 1691.90(15) $Å^3$ |
| Z | 2 | 4 |
| Density (calculated) | 1.378 g/cm3 | 1.273 $g/cm^3$ |
| Absorption coefficient | 0.198 mm-1 | 0.086 $mm^{-1}$ |
| F(000) | 414 | 688 |
| Crystal size | 0.180 x 0.220 x 0.250 mm | 0.130 x 0.220 x 0.250 mm |
| Theta range for data collection | 1.45 to 24.99° | 2.21 to 25.00° |
| Index ranges | -7<=h<=7, -12<=k<=12, -17<=l<=17 | -11<=h<=9, -10<=k<=12, -20<=l<=19 |
| Reflections collected | 12174 | 12531 |
| Independent reflections | 3333 [R(int) = 0.0184] | 2973 |
| Completeness to theta | 99.8% | 99% |
| Absorption correction | multi-scan | multi-scan |
| Max. and min. transmission | 0.9650 and 0.9520 | 0.9650 and 0.9520 |
| Refinement method | Full-matrix least-squares on $F^2$ | Full-matrix least-squares on $F^2$ |
| Data / restraints / parameters | 3333 / 0 / 260 | 2973 / 0 / 226 |
| Goodness-of-fit on F2 | 1.053 | 1.032 |
| Final R indices [I>2sigma(I)] | 3016 data; I>2σ(I)R1 = 0.0415, wR2 = 0.1106all | 2160 data; I>2σ(I)R1 = 0.0415, wR2 = 0.1106all |
| R indices (all data) | R1 = 0.0458, wR2 = 0.1157 | R1 = 0.0637, wR2 = 0.1199 |
| Largest diff. peak and hole | 0.557 and -0.630 $eÅ^{-3}$ | 0.255 and -0.216 $eÅ^{-3}$ |

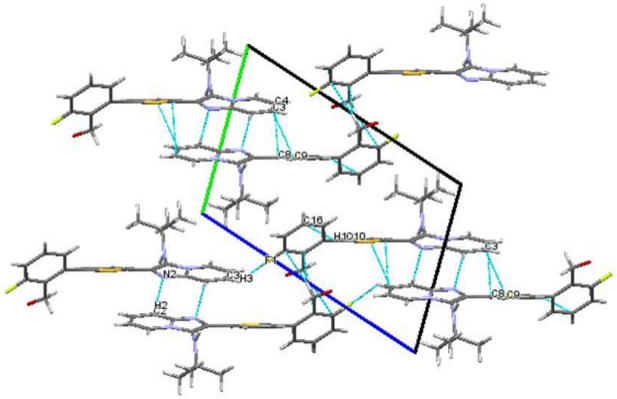

**Fig. 3: The crystal packing of compound I showing the intermolecular interactions**

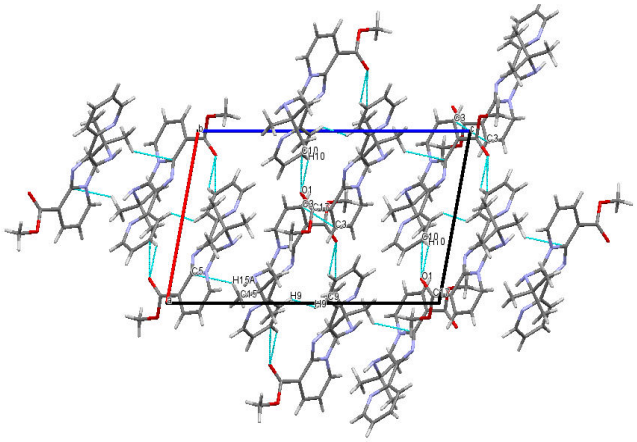

**Fig. 4: The crystal packing of compound II showing the intermolecular interactions**

**Table 2: Selected Bond lengths [Å] for Compound I and II**

| Compound I | | Compound II | |
|---|---|---|---|
| Bond | Bond length [Å] | Bond | Bond length [Å] |
| C1-N2 | 1.327(2) | C1-C2 | 1.342(3) |
| C1-C2 | 1.413(3) | C4-C17 | 1.479(2) |
| C6-N3 | 1.388(2) | C5-N1 | 1.399(2) |
| C7-N2 | 1.374(2) | C6-N2 | 1.384(2) |
| C8-C9 | 1.364(3) | C7-N1 | 1.388(2) |
| C9-C10 | 1.405(3) | C8-N3 | 1.344(2) |
| C10-C11 | 1.362(3) | C9-C10 | 1.374(3) |
| C11-C12 | 1.473(2) | C10-C11 | 1.368(3) |
| C12-C17 | 1.396(3) | C11-C12 | 1.370(3) |
| C13-C14 | 1.391(3) | C12-N3 | 1.340(2) |
| C14-F1 | 1.353(2) | C13-C16 | 1.493(3) |
| C15-C16 | 1.378(3) | C13-N4 | 1.506(2) |
| C16-C17 | 1.378(3) | C17-O2 | 1.334(2) |
| C18-C19 | 1.518(3) | C1-N1 | 1.376(2) |
| C18-C21 | 1.524(3) | C2-C3 | 1.412(3) |
| C22-O1 | 1.195(3) | C3-C4 | 1.368(3) |
| C1-N1 | 1.385(2) | C4-C5 | 1.427(2) |
| C2-C3 | 1.358(3) | C5-N2 | 1.317(2) |
| C3-C4 | 1.415(3) | C6-C7 | 1.378(2) |
| C4-C5 | 1.349(3) | C6-C8 | 1.466(2) |
| C5-N1 | 1.380(2) | C7-N4 | 1.398(2) |
| C6-C7 | 1.380(2) | C8-C9 | 1.378(3) |
| C6-N1 | 1.397(2) | C13-C15 | 1.501(3) |
| C7-C8 | 1.456(2) | C13-C14 | 1.510(3) |
| C8-S1 | 1.7264(17) | C17-O1 | 1.202(2) |
| | | C18-O2 | 1.447(2) |

## 3. RESULTS AND DISCUSSION

### 3.1. X-ray crystallographic studies

The compound I consists of a imidazole, pyridine, sulphur and benzene ring with a O1 chain connected at C22 position of the benzene ring and N3/C18-C21 chain connected at C6 of the imidazole ring. Flourine atom is connected at C14, whereas in compound II O1 chain is connected to C4 of the imidazole ring. The pyridine ring (C1-C5/N1) is fused with the imidazole ring making a dihedral angle of 1.51(10)° and 8.89(9) in compound I and II respectively. The dihedral angle between the pyridine and the benzene rings is 59.28(10) and between the atoms S1/C8-C11 and the imidazole ring is 17.43(3)° in compound I. The dihedral angle between the Imdiazole ring and N3/C8-C12 is 14.43(8).

The sum of bond angles around N1 are 360° and 359.3°in compound I and II which confirms that the atom N1 is in $sp^2$hybridized state [27]. In compound I atom C18 and in compound II C13 has a tetrahedral configuration with angles (C20-C18-N3 = 107.21(18)° C15-C13-N4=105.63° and C21-C18-C19 =108.94 (19)° C14-C13-C16= 110.4(2). The torsion angles for Compound I for the atoms C20-C18-N3-C6 and C16-C17-C12-C11 are 162.59 (3)° and 176.74(19)° respectively, in Compound II for the atoms C18-O2-C17-C4= 178.54(16)° and C15-C13-N4-C7=-175.93 (18)° respecttively. In compound I, molecules are linked by intermolecular C2-H2...N2 hydrogen bonds as shown in Fig. 3. The molecule also exhibits π...π and C-H...π interactions. In compound II, molecules are linked by intermolecular N(4)-H(1N)...N(3) and C(10)-H(10)...O(1) hydrogen bonds as shown in Fig. 4. The chains are linked by C-H...π interactions.

**Table 3: Selected bond angles [Å] for Compound I and Compound II**

| | Bond Angle [°] | Bond | Bond Angle [°] | Bond | Bond Angle [°] | Bond | Bond Angle [°] |
|---|---|---|---|---|---|---|---|
| N1-C1-C2 | 111.03(15) | C7-C8-S1 | 118.23(13) | C2-C1-N1 | 119.31(17) | C1-C2-C3 | 120.56(18) |
| C3-C2-H2 | 118.54(16) | C9-C10-H10 | 123.1 | N1-C1-H1 | 120.3 | C3-C2-H2 | 119.7 |
| C2-C3-C4 | 120.4 | C17-C12-C13 | 119.17(17) | C1-C2-H2 | 119.7 | C4-C3-H3 | 119.4 |
| C4-C3-H3 | 120.56(18) | C13-C12-C11 | 121.69(17) | C4-C3-C2 | 121.21(18) | C3-C4-C5 | 118.47(16) |
| C5-C4-H4 | 119.7 | C14-C13-C22 | 121.60(18) | C2-C3-H3 | 119.4 | C5-C4-C17 | 119.04(16) |
| C4-C5-N1 | 119.6 | F1-C14-C15 | 117.14(18) | C3-C4-C17 | 122.35(17) | N2-C5-C4 | 130.91(16) |
| N1-C5-H5 | 118.72(18) | C15-C14-C13 | 124.03(19) | N2-C5-N1 | 111.26(15) | C7-C6-N2 | 111.47(16) |
| N2-C7-C6 | 120.6 | C14-C15-H15 | 121 | N1-C5-C4 | 117.70(15) | N2-C6-C8 | 120.20(15) |
| C6-C7-C8 | 112.14(15) | C17-C16-C15 | 120.8(2) | C7-C6-C8 | 128.00(16) | N3-C8-C9 | 122.14(18) |
| C9-C8-S1 | 129.11(16) | C15-C16-H16 | 119.6 | N1-C7-N4 | 121.10(15) | C9-C8-C6 | 120.49(17) |
| C8-C9-C10 | 110.42(13) | C16-C17-H17 | 119.5 | N3-C8-C6 | 117.29(16) | C10-C9-H9 | 120.1 |
| C10-C9-H9 | 113.28(17) | C19-C18-C20 | 110.13(19) | C10-C9-C8 | 119.8(2) | C11-C10-C9 | 118.6(2) |
| C11-C10-H10 | 123.4 | O1-C22-C13 | 124.5(2) | C8-C9-H9 | 120.1 | C9-C10-H10 | 120.7 |
| C10-C11-C12 | 123.1 | C5-N1-C1 | 122.20(15) | C11-C10-H10 | 120.7 | C10-C11-H11 | 120.7 |

| | | | | | | | |
|---|---|---|---|---|---|---|---|
| C12-C11-S1 | 129.43(17) | C6-N3-C18 | 120.86(15) | C10-C11-C12 | 118.5(2) | N3-C12-C11 | 124.2(2) |
| C17-C12-C11 | 120.28(13) | C18-N3-H1N | 117.6(19) | C12-C11-H11 | 120.7 | C11-C12-H12 | 117.9 |
| C14-C13-C12 | 119.08(17) | C12-C17-H17 | 119.5 | N3-C12-H12 | 117.9 | C16-C13-C14 | 110.3(3) |
| C12-C13-C22 | 117.02(18) | C5-N1-C6 | 130.18(16) | O1-C17-O2 | 123.20(18) | N4-C13-C14 | 112.01(17) |
| F1-C14-C13 | 121.33(17) | C6-N3-H1N | 118.6(19) | O2-C17-C4 | 111.97(17) | O1-C17-C4 | 124.79(18) |
| C14-C15-C16 | 118.79(19) | N2-C1-C2 | 130.43(17) | C1-N1-C5 | 122.27(15) | C1-N1-C7 | 130.16(15) |
| C16-C15-H15 | 118.03(19) | C3-C2-C1 | 119.13(19) | C7-N4-C13 | 118.16(14) | C12-N3-C8 | 116.71(17) |

**Table 4: Selected Torsion angles [Å] for Compound I and II**

| COMPOUND I | | COMPOUND II | |
|---|---|---|---|
| BOND | TORSION ANGLE [°] | BOND | TORSION ANGLE [°] |
| N2-C1-C2-C3 | -179.89(19) | C3-C4-C5-N2 | 167.76(18) |
| N1-C6-C7-C8 | -178.83(17) | N2-C6-C7-N4 | 178.80(18) |
| C6-C7-C8-S1 | -164.12(15) | C7-C6-C8-C9 | -178.36(19) |
| C9-C10-C11-C12 | 175.53(19) | C5-C4-C17-O2 | 148.36(16) |
| C17-C12-C13-C22 | -177.28(18) | N4-C7-N1-C5 | -179.79(15) |
| C12-C13-C14-F1 | -178.30(17) | C4-C5-N1-C7 | 179.12(15) |
| F1-C14-C15-C16 | 178.8(2) | C4-C5-N2-C6 | -176.32(18) |
| N2-C1-N1-C5 | -177.77(15) | C8-C6-N2-C5 | 172.15(16) |
| C7-C6-N1-C5 | 177.47(16) | C4-C17-O2-C18 | 178.53(15) |
| C7-C8-S1-C11 | -178.03(15) | C8-C6-C7-N1 | -169.85(17) |
| C12-C11-S1-C8 | -176.03(16) | N2-C6-C8-N3 | -168.02(16) |
| N3-C6-C7-N2 | -175.88(18) | C6-C8-C9-C10 | -177.9(2) |
| N2-C7-C8-C9 | -160.75(19) | C3-C4-C17-O1 | 141.6(2) |
| C7-C8-C9-C10 | 177.03(19) | C2-C1-N1-C7 | -172.06(17) |
| C11-C12-C13-C14 | -176.97(17) | C6-C7-N1-C1 | 166.70(17) |
| C22-C13-C14-C15 | 177.1(2) | N2-C5-N1-C1 | -168.47(15) |
| C11-C12-C17-C16 | 176.75(19) | C6-C8-N3-C12 | 178.68(17) |
| C4-C5-N1-C6 | 178.78(17) | C15-C13-N4-C7 | -175.9(2) |
| C2-C1-N1-C6 | -178.51(15) | | |
| N3-C6-N1-C1 | 176.30(15) | | |

**Table 5: Hydrogen bonds for the Compound I [Å ]**

| D-H…A | d(D-H) | H···A | D···A | D-H···A |
|---|---|---|---|---|
| C17-H17…S1 | 0.93 | 2.87 | 3.194(2) | 102 |

*Symmetry codes 1+x,1-y, z*

**Table 6: Hydrogen bonds for the Compound II [Å ]**

| D-H…A | d(D-H) | H···A | D···A | D-H···A |
|---|---|---|---|---|
| N(4)-H(1N)…N(3) | 0.86(2) | 2.39(2) | 3.026(2) | 131.2(17) |
| C(10)-H(10)…O(1) | 0.93(2) | 2.50(2) | 3.212(3) | 133 |

*Symmetry codes 1+x,1-y, z*

### 3.2. Hirshfeld surface analysis

Hirshfeld surface analysis was done using crystal Explorer 17.5 software [28], which identifies the nature of interaction and proportion of the molecule inside the crystal. In compound I, C–H···S interactions can be identified by large red spots, and the small red spots on surfaces indicate the C–H···F and C–H···N interactions as shown in Fig 6. In compound II, N-H…N and C-H…O hydrogen bonds are identified by red spots as shown in Fig 7. The expanded 2D fingerprint plots [29-30] were drawn in the $d_e$ and $d_i$ as graph axes. Here $d_e$ and $d_i$ are the distances to the nearest nuclei outside and inside the surface from the Hirshfeld surface respectively. Fig.6a-6d & 7a-7d shows the view of the Hirshfeld surface mapped over $d_{norm}$, shape index, curvature and fragment patches. The π-π stacking

interaction arrangements are clearly shown by the shape index and curvedness surfaces. The red and blue triangles in the shape index indicate the π-π interactions present in the crystal structure. The curvedness surface indicates the electron density surface curves around the molecular interactions [31].

Fig. 8 & Fig 9 show the two-dimensional fingerprint plots. The H···H interaction shows a major contribution (43.1%) in compound I and 53.8% in compound II to the total Hirshfeld surface. The C–H···π interactions comprise 21.6% in compound I, 21.7% in compound II of the total Hirshfeld surface, and the π···π interaction contributes 2.9% in compound I, 1.4 %in compound II to the total Hirshfeld surface. These interactions are accordance with the results of the single crystal XRD.

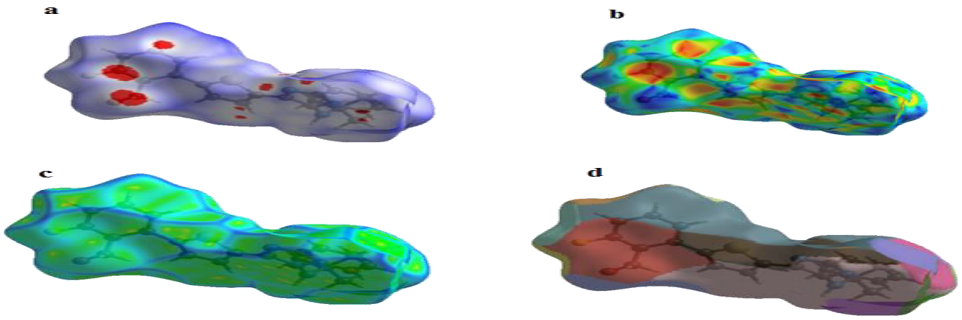


**Fig. 6: View of the Hirshfeld surface mapped over a) $d_{norm}$ b) shape index c) curvature d) fragment patches for compound I**

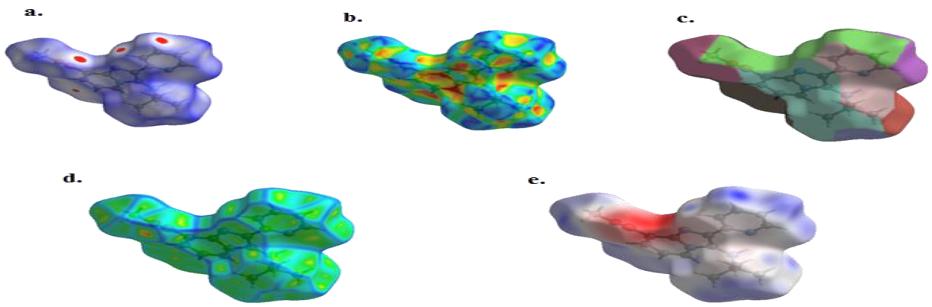


**Fig. 7: View of the Hirshfeld surface mapped over a) $d_{norm}$ b) shape index c) fragment patches d) curvature e) electrostatic potential for compound II**

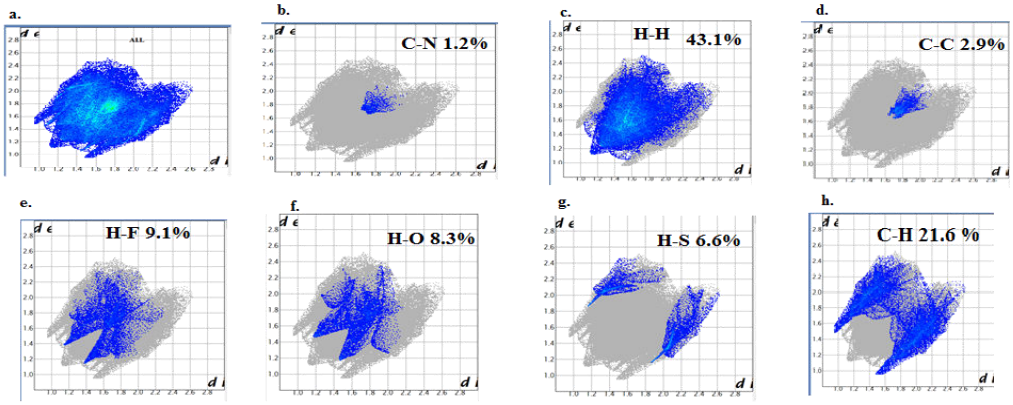


**Fig. 8: The two-dimensional fingerprint plots for (*a*) all interactions, (*b*) C…N, (*c*)H…H,(*d*)C…C (*e*) H…Fand (*f*) H…O interactions (g)H…S (h) C…H**

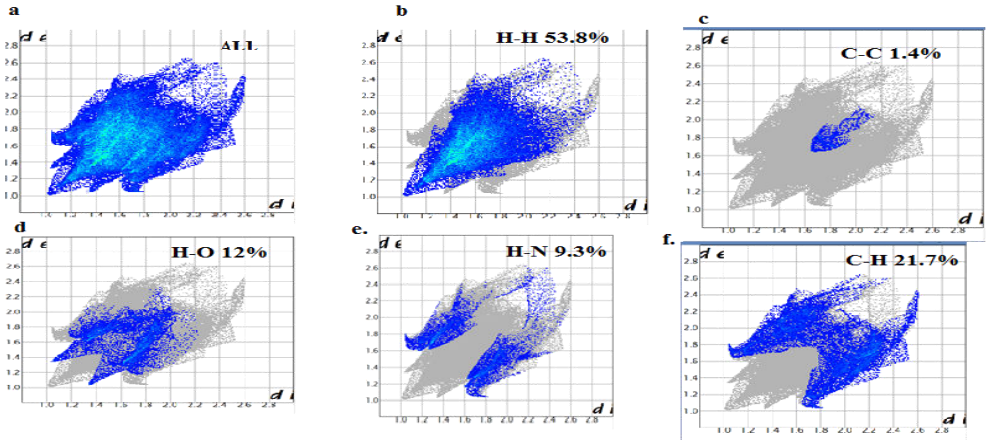


**Fig. 9: The two-dimensional fingerprint plots for (*a*) all interactions, (*b*) H…H (c) C…C, (d)H…O,(*d*) (*e*) H…N and (*f*) C…H interactions**

### 3.3. Energyframework analysis

The monomer wavefunctions at the HF/3-21G level was used to find the interaction energies between the molecules. A 3.8Å radius cluster of molecules around the selected molecule was created to calculate the total interaction energy. The scale factors used in the CE … HF/3-21G electron densities benchmarked energy model [32] are given in Table 7. The energies calculated by the energy model reveals that the dispersion energy contributes significantly to the interactions in the crystal (table 8 and 9).

A cluster of molecules present in 2 x 2 x 2 unit cells were used for energy framework calculation using the CE-HF/3-21G energy model. The total interaction energy is given as $E_{tot}=k_{ele}E_{ele}+k_{pol}E_{pol}+k_{dis}E_{dis}+k_{rep}E_{rep}$ where the k values are scale factors. $E_{ele}$ represents electrostatic component, $E_{pol}$ represents the polarization energy, $E_{dis}$ represents the dispersion energy, and $E_{rep}$ represents the exchange-repulsion energy [33].

The interaction energies calculations are shown in table from which we can say that the dispersion energy framework is dominant over electrostatic energy framework. Fig.10 and 11 shows the energy framework diagram for compound I and II. The supramolecular architecture of the crystal structures are visualized uniquely by energy frameworks.

**Table 7: Scale factors for benchmarked energy model.**

| Energy Model | k_ele | k_pol | k_disp | k_rep |
|---|---|---|---|---|
| CE-HF … HF/3-21G electron densities | 1.019 | 0.651 | 0.901 | 0.811 |

**Table 8: Interaction energies (kJ mol_1) for compound I**

| N | Symop | R | $E_{\_ele}$ | $E_{\_pol}$ | $E_{\_dis}$ | $E_{\_rep}$ | $E_{\_tot}$ |
|---|---|---|---|---|---|---|---|
| 2 | x, y, z | 15.94 | -5.1 | -1.1 | -7.7 | 2.3 | -10.9 |
| 1 | -x, -y, -z | 10.33 | -1.9 | -2.4 | -39.9 | 37.8 | -8.8 |
| 2 | x, y, z | 6.63 | -19.7 | -7.1 | -52.8 | 27.4 | -49.9 |
| 1 | -x, -y, -z | 9.16 | -22.2 | -7.8 | -22.3 | 15.5 | -35.3 |
| 1 | -x, -y, -z | 8.02 | -6.2 | -2.1 | -46.3 | 19.6 | -33.5 |
| 1 | -x, -y, -z | 7.60 | -8.6 | -1.8 | -40.0 | 15.4 | -33.5 |
| 2 | x, y, z | 15.14 | -8.2 | -2.5 | -8.2 | 3.4 | -14.6 |
| 1 | -x, -y, -z | 10.28 | -5.3 | -3.2 | -15.8 | 5.9 | -16.9 |
| 1 | -x, -y, -z | 8.01 | -11.9 | -8.0 | -79.8 | 42.7 | -54.7 |
| 1 | -x, -y, -z | 11.43 | -4.9 | -1.0 | -29.1 | 13.3 | -21.1 |
| 1 | -x, -y, -z | 13.88 | 1.9 | -0.7 | -15.4 | 6.2 | -7.3 |
| | Total Energy | | -92.1 | -37.7 | -357.3 | 189.5 | -286.5 |

**Table 9: Interaction energies (kJ mol_1) for compound II**

| N | Symop | R | E_ele | E_pol | E_dis | E_rep | E_tot |
|---|---|---|---|---|---|---|---|
| 2 | -x+1/2, y+1/2, -z+1/2 | 12.48 | 0.2 | -0.3 | -8.4 | 2.4 | -5.6 |
| 1 | -x, -y, -z | 8.37 | -24.7 | -12.3 | -32.1 | 22.2 | -44.0 |
| 1 | -x, -y, -z | 7.91 | -11.1 | -2.1 | -50.0 | 25.6 | -36.9 |
| 1 | -x, -y, -z | 5.93 | -8.4 | -6.8 | -44.0 | 14.2 | -41.1 |
| 2 | -x+1/2, y+1/2, -z+1/2 | 7.23 | -3.1 | -2.2 | -40.0 | 16.6 | -27.3 |
| 2 | x, y, z | 9.90 | -0.5 | -1.6 | -21.1 | 5.9 | -15.8 |
| 2 | x, y, z | 10.33 | 0.1 | -0.4 | -6.9 | 0.7 | -5.8 |
| 2 | x+1/2, -y+1/2, z+1/2 | 10.72 | -6.6 | -1.7 | -14.6 | 5.1 | -16.8 |
| 1 | -x, -y, -z | 9.88 | -9.4 | -3.4 | -25.6 | 8.8 | -27.7 |
| | Total | | -63.5 | -30.8 | -242.7 | 101.5 | -221 |

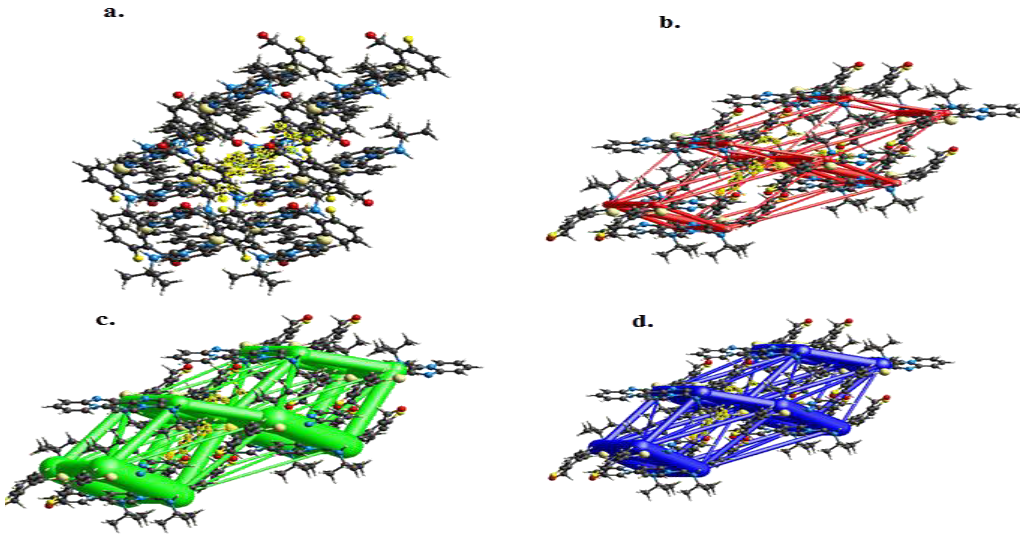


**Fig. 10: a) Interaction between the selected molecule and the molecules present in a 3.8 A ° cluster around it, (b) Coulombic energy, (c) dispersion energy and (d) total energy.**

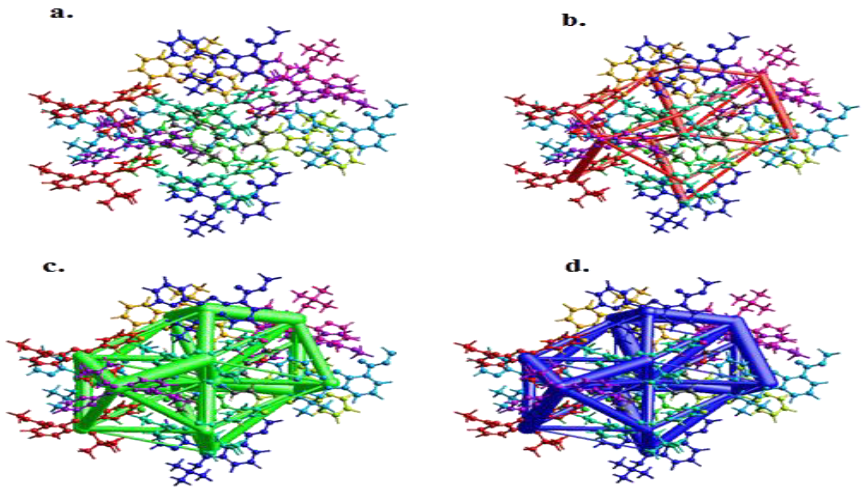


**Fig. 11: a) Interaction between the selected molecule and the molecules present in a 3.8 A ° cluster around it, (b) Coulombic energy, (c) dispersion energy and (d) total energy.**

## 4. CONCLUSIONS

Two novel compounds of imidazole derivative were synthesized and obtained by slow evaporation from ethyl alcohol (EtOH) solution at room temperature. The crystal structures were stabilized by the two kinds of offset π···π stacking and C…H…π interaction. The geometrical results of the compounds are in good agreement with the X-ray crystallographic data and Hirshfeld surface analysis. The π-π stacking interactions are confirmed by shape index and curvedness of Hirshfeld surface. The intermolecular contacts obtained by Hirshfeld analysis substantiate the XRD results. The energies calculated by the energy model reveals that the dispersion energy contributes significantly to the interactions.

Supplementary crystallographic data were deposited in CCDC (Cambridge Crystallographic Data Centre, No: 1920810, 1920813). The data can be acquired free of charge via http:/www.ccdc.cam.ac.uk/conts/retrieving. html, or e-mail: deposit@ccdc.ac.uk.

## 5. REFERENCES


1. Desiraju GR, Vittal JJ, Ramanan J. *Crystal Engineering: A Textbook* World Scientific Singapore, 2012; 3574.
2. Desiraju GR. *J. Am. Chem.* Soc., 2013; **135:**9952.
3. Desiraju GR. *Angew.Chem. Int. Eds*., 2007; **46**:8342.
4. Czarnik A. *Guest Editorial Acc. Chem. Res*., 1996; **29:** 112-113.
5. Banfi E, Scialino G, Zampieri D, Mamolo MG, Vio L , Ferrone M, et al. *J. Antimicrob.Chemother*., 2006; **58:**76-84.
6. Jackson CJ, Lamb DC, Kelly DE, Kelly SL. *FEMS Microbiol.Lett.,* 2000; **192:**159-162.
7. Dooley SW, Jarvis WR, MartoneWJ, Snider DE. *Intern. Med.* 1992; **117**:257-259.
8. Cui B, Zheng BL, He K, Zheng QYJ. *Nat. Prod*., 2003; **66:**1101-1103.
9. Biftu T, Feng D, Fisher M, Liang GB , Qian X , Scribner A, et al. *Med. Chem. Lett.,* 2006; **16**:2479-2483.
10. Gudmundsson KS, Johns BA. *Bioorg.Med. Chem. Lett.* 2007; **17:**2735-2739.
11. Rupert KC, Henry JR, Dodd JH, Wadsworth SA, Cavender DE, Olini GC, et al. *Bioorg.Med.Chem. Lett.,* 2003; **13:**347-350.
12. Spasov AA, Yozhitsa IN, Bugaeva LI, Anisimova VA. *Pharm. Chem. J*., 1999; **33**:232-243.
13. Gueiffier A, Mavel S, Lhassani M, Elhakmaoui A, Snoeck R, Andrei G, et al. *J. Med. Chem*. 1998; **41:**5108-5112.
14. Jain R, Jain S, Gupta RC, Anand N, Dutta GP, Puri SK. *Indian J. Chem.,*1994*;* **338**:251.
15. Mohammed A, Abdel-Hamid N, Maher F, Farghaly A Czech. *ChemCommun.,* 1992; **57(7):**1547.
16. Rajat Ghosh, Biplab De. *J. Pharm. Sci. Rev. Res.,* 2013; **23(2):**237-246.
17. Delia Hernández Romero, Víctor E, Torres Heredia, Oscar García-Barradas, Ma. Elizabeth MárquezLópez, Esmeralda Sánchez Pavón. *J. of Chem. and Biochem.,* 2014; **2(2):**45-83.
18. Nakamura T, Nakamura K, Hayashi H. *Photographic element*,1988; EP0160947 **(B1).**
19. Clark B, Allway P, Zuberi T, Singer S, Heckler C, Friedrich L. 2005;**WO2005/036262.**
20. Hartmann H, Zeika O, Ammann M, Dathe R. 2010; **US2010/0301277A1**.
21. Blessing RH. *ActaCrystallographica Sect A*., 1995; **51:**33.
22. Dhanalakshmi G, Mala Ramanjaneyulu, Sathiah Thennarasu, Aravindhan S. *ActaCryst. E* 2018; **74**:1913-1918.

22a. Mala R, Suman K, Nandhagopal M, Narayanasamy M, Thennarasu S. *SpectrochimicaActa Part A: Molecular and Biomolecular Spectroscopy*, 2019; **222**:117236.

22b. Mala R, Nandhagopal M, Narayanasamy M, Thennarasu S. *ChemistrySelect*., 2019; **4(45)**:13131-13137.

23. SheldrickGM. *ActaCryst.A*., 2015a**71**:3-8.
24. Sheldrick GM. *Acta Cryst.C.,* 2015;**71:**3-8.
25. Spek AL. *ActaCrystA.,* 1990; **46**:c34.
26. Macrae CF, Bruno IJ, Chisholm JA, Edgington PA, McCabe PA, Pidcock A, et al. *J. Appl. Cryst*., 2008; **41:**466-470.
27. Beddoes RL, Dalton L, Joule TA, Mills OS, Street JD, Watt CI. *J. Chem. Soc. Perkin trans.*. 1986; **2:**787.
28. Wolff SK, Grimwood DJ, McKinnon JJ, Jayatilaka JJ, Spackman MA. *Crystal Explorer 3.0* University of Western Australia Perth Australia, 2001.
29. Seth SK. *J. Mol. Stru.,* 2014; **1064**:70-75.
30. McKinnon JJ, Jayatilaka D, Spackman MA. *Chem. Com*., 2007; **37:**3814-3816.
31. Meenatchi R, Agilandeshwari S, Meenakshisundaram P. *RSC Adv*., 2015; 571076-571087.
32. Mackenzie CF, Spackman PR, Jayatilaka D, Spackman MA. *IUCrJ* ., 2017; **4**:575-587.
33. Turner MJ, Grabowsky S, Jayatilaka D, Spackman MA. *J. Phys. Chem. Lett.,* 2014; **5**:4249-4255.